Adsorption and cake layer fouling in relation to Fenton cleaning of ceramic nanofiltration membranes

Lin, Bin; Rietveld, Luuk C.; Yao, Lu; Heijman, Sebastiaan G.J.

DOI
10.1016/j.memsci.2023.122097

Publication date
2023

Document Version
Final published version

Published in
Journal of Membrane Science

Journal of Membrane Science 687 (2023) 122097

Contents lists available at ScienceDirect

Journal of Membrane Science

journal homepage: www.elsevier.com/locate/memsci

Adsorption and cake layer fouling in relation to Fenton cleaning of ceramic nanofiltration membranes

Bin Lin [a,b,*], Luuk C. Rietveld [a], Lu Yao [a], Sebastiaan G.J. Heijman [a]

[a] Department of Water Management, Faculty of Civil Engineering and Geosciences, Delft University of Technology, Stevinweg 1, 2628, CN Delft, the Netherlands
[b] State Key Laboratory of Materials-Oriented Chemical Engineering, National Engineering Research Center for Special Separation Membrane, Nanjing Tech University, Nanjing, 210009, China

ARTICLE INFO

Keywords:
Ceramic membrane
Nanofiltration
Adsorptive fouling
Cake layer
Fenton cleaning

ABSTRACT

Catalytic ceramic nanofiltration (NF) is a promising technology for direct wastewater reclamation, given its high separation selectivity and reactive surfaces for oxidative removal of fouling. A better understanding of the relation between fouling types and oxidative cleaning efficacy under high organic loading conditions is of practical importance for realizing stable filtration/cleaning performance in long-term water reclamation operations. In this work, Fenton cleaning, using a hydrogen peroxide solution and an iron oxychloride catalyst precoat layer on top of commercially available ceramic NF membranes, was studied with respect to high organic loaded fouling, simulated by a concentrated sodium alginate solution in the presence of calcium. Adsorption (in the absence of a permeate flow) and constant-pressure filtration (with a permeate flow) experiments were performed to distinguish between permeance decreases as a result of either adsorptive or cake layer fouling. The results show that the flux evolution could be divided into an initial sharp flux decline, due to rapid adsorption of the foulants, and a subsequent gradual flux decrease, resulting from progressive cake build-up on the membrane. The two-stage flux decrease was enhanced during the constant-pressure filtration experiments, because they start at a high flux with a high fouling rate, while the flux gradually decreases as fouling proceeds. During multiple adsorption/cake filtration/Fenton cleaning cycles, the cake layer fouling was sufficiently removed by Fenton cleaning in contrast to the adsorptive fouling. However, the total permeate production during ceramic NF was not influenced by the remaining adsorptive fouling (after cleaning), since the adsorptive fouling always only occurs at the beginning of each cycle. The findings provide new insights into the criteria for evaluating and optimizing the efficacy of oxidative (Fenton) cleaning during ceramic NF in water treatment.

1. Introduction

Direct nanofiltration (NF) is a promising technique for wastewater reclamation without any pre-treatment, given its potential in simplifying the operations, in particular, during small-scale water recycling applications. NF processes typically enable the removal of most organic matter, a fraction of hardness-causing compounds and multivalent ions, and almost all microbes from wastewater via size exclusion and/or electrostatic repulsion [1,2]. However, the most used polymeric spiral-wound membranes are susceptible to biofouling and spacer clogging by colloids at high concentrations in wastewater [3,4]. As an alternative, commercial composite polyamide NF membranes can only be applied at a very low permeate flux (e.g. 3 L m^{-2} h^{-1}) to maintain steady performance during direct NF treatment of secondary wastewater effluent [5].

Ceramic NF has emerged as a potential substitute for polymeric NF in direct wastewater reclamation applications, owing to its greater durability against harsh operating environments and better adaptability to high organic loading. Cabrera et al. reported that commercial ceramic NF was able to directly treat industrial wastewater with high organic loading varying from 30 to 135 mg L^{-1} in a pilot operation for two years [6,7]. As demonstrated by Lee et al. [8], a rejection of 60–98% of humic acid and colloids was attained during ceramic NF of model semiconductor wastewater, notwithstanding its high organic loading of 58.4 mg L^{-1}. In addition, according to Mustafa et al. [9] and Kramer et al. [10], stable filtration performance could be maintained at an operating

* Corresponding author. Department of Water Management, Faculty of Civil Engineering and Geosciences, Delft University of Technology, Stevinweg 1, 2628, CN Delft, the Netherlands.
E-mail addresses: b.lin@tudelft.nl, binlin-1@outlook.com (B. Lin).

https://doi.org/10.1016/j.memsci.2023.122097
Received 26 April 2023; Received in revised form 30 August 2023; Accepted 15 September 2023
Available online 16 September 2023

flux of above 15–50 L m^{-2} h^{-1} during direct ceramic NF of oily wastewater and municipal sewage for water reclamation. However, membrane fouling, in particular, by a thick and compact cake layer, formed during filtration with organic molecules/colloids at high concentrations, is a critical obstacle for upscaling ceramic NF membranes to the industrial implementation in direct wastewater reclamation [10,11]. Forward flush is not effective enough to remove the sticky cake layer [9,12]. Hydraulic backwash at high backwash pressures damages the sealing at both ends of tubular ceramic NF membranes, resulting in the formation of defects on the membrane surface [13]. Chemical cleaning with sodium hypochlorite or caustic soda/citric acid is able to restore the permeate flux during ceramic NF, but it causes enlargement of the membrane pores [14,15].

Catalytic ceramic membranes, functionalizing the membrane surface with oxidative reactivity, provide a potential oxidation route for fouling removal. Over the past decade, several advanced oxidation processes, including Fenton reactions [16,17], catalytic ozonation [18,19], peroxymonosulfate activation [20,21] and photo-catalysis [22], have tentatively been incorporated in catalyst-tailored ceramic membranes to produce reactive oxygen species (e.g. $^{\bullet}OH$, $O_2^{\bullet-}$ and $SO_4^{\bullet-}$ radicals) on the membrane surface and/or within the inner pores, potentially removing fouling. Angelis et al. observed that the flux recovery of iron-oxide coated ceramic membranes (fouled with humic acids) by Fenton cleaning, was much higher (97%) than those by forward flush (41%) or acidic/caustic cleaning (39–42%) [17]. Zhang et al. demonstrated that the flux of MnO_2–Co_3O_4 coated ceramic membranes was recovered by 97% with peroxymonosulfate-based oxidative cleaning, while it was only restored by 70–75% using backwash or acidic/caustic cleaning [23]. However, present knowledge about catalytic ceramic membranes, regarding their fouling characteristics and oxidative cleaning effectiveness, is mainly limited to ceramic microfiltration and ultrafiltration processes, and not to ceramic NF. In particular, a better understanding of the fouling characteristics during ceramic NF with high organic loaded wastewater and their influence on oxidative cleaning efficacy is still lacking.

Fouling of ceramic NF by soluble and colloidal biopolymers (e.g. polysaccharide) has been considered a multifaceted process, involving adsorption, pore constriction/blockage and cake development [12,24]. Fujioka et al. reported that the increase in transmembrane pressure (TMP) during ceramic NF of wastewater was reduced by about 60% via ozonated water flush, but it remained unclear how the ozonation cleaning corresponded to, or was influenced by, different fouling pathways [11]. As an indication of multiple fouling pathways, a two-stage flux decrease pattern, comprising a rapid decline in permeation flux at the early stage of filtration and a gradual flux decline afterwards, has previously been recognized for ceramic NF membranes, during constant pressure experiments, presumably resulting from strong foulant-membrane interactions (e.g. polar and electrostatic interactions) or a high starting flux [9,12]. Besides, a recent study presented a steep flux decline (30–40%), occurring upon switching the feed from pure water to an alginate solution during ceramic NF [25]. Nonetheless, the exact reason for the rapid flux decline and how it affects cleaning performance are still unanswered. Kramer et al. observed a flux recovery of 75% by Fenton cleaning over an iron-oxide coated ceramic NF membrane fouled by alginate, however, the sharp flux decline relative to the initial clean water flux was not taken into account [13].

Therefore, the objective of this study was to distinguish between multiple types of organic fouling in relation to their impact on Fenton cleaning efficacy of catalyst pre-coated ceramic NF membranes. Iron oxychloride (FeOCl), a reactive heterogeneous Fenton catalyst, was pre-coated on top of a commercial ceramic (TiO_2) NF membrane, for catalysing the in-situ decomposition of hydrogen peroxide (H_2O_2) into hydroxyl radicals ($^{\bullet}OH$) on the membrane surface [26–28]. Sodium alginate was employed as a typical surrogate for extracellular polymeric substance, identified as the major fouling-causing substance in domestic wastewater [29–31]. A concentrated alginate solution (0.8 g L^{-1}) in the presence of calcium ions was adopted to promote the formation of a thick and compact cake layer on the FeOCl pre-coated membrane, for examining the concept of direct water reclamation from high organic loaded wastewater. Angelis et al. have compared the morphology of organic fouling on an iron oxide coated ceramic membrane by alginate, bovine serum albumin and humic acid, respectively, demonstrating that only the alginate foulant could form thick cake layer fouling on the pre-coat layer while the other two foulants partially blocked its pores without any cake build-up [17,32]. Additionally, as suggested by Katsoufidou et al. [33] and Kim et al. [34], alginate solutions in the presence of calcium consist of both soluble organic matter and large-sized colloids, which are thus assumed to cause adsorptive fouling (or pore blocking) and cake layer fouling, respectively. Hence, alginate was considered as the proper foulant surrogate in this study, where a simulation and differentiation of the multiple fouling types were needed for the aforementioned research objective. Flux restoration percentages, determined in terms of both pure water flux and foulant solution flux, were used as an indication for oxidative cleaning efficacy and evaluated in relation to the various fouling types of the FeOCl pre-coated membrane in a constant-pressure filtration mode.

2. Materials and methods

2.1. Reagents and materials

Ferric chloride hexahydrate ($FeCl_3 \bullet 6H_2O$, ≥99.0%) and sodium alginate (≥99.0%) were purchased from Sigma-Aldrich. Calcium chloride dihydrate ($CaCl_2 \bullet 2H_2O$, ≥99.0%) and H_2O_2 (30%) were purchased from Merck KGaA (Germany). All chemicals were used as received. Ceramic NF membranes (Inopor GmbH, Germany) with a mean pore size of 0.9 nm (Inopor data) were used in this study. The membranes have a tubular single-channel configuration (outer diameter: 10 mm, inner diameter: 7 mm, length: 100 mm) with the separation layer made of TiO_2. Both ends of the tubular membranes were sealed with silica glass. The membranes were operated in an inside-out filtration mode.

2.2. Preparation of FeOCl catalyst and FeOCl pre-coated membrane

The FeOCl catalyst was synthesized through a thermal annealing method [28]. $FeCl_3 \bullet 6H_2O$ powder (10.0 g), as the precursor, was heated in a sealed crucible at a heating rate of 20 °C min^{-1} to 220 °C and remained for 1 h in a muffle furnace. The reaction equation is presented in Eq. (1).

$$FeCl_3 \bullet 6H_2O \rightarrow FeOCl + 2HCl + 5H_2O \quad (1)$$

The FeOCl suspension was prepared by dispersing 4.0 g of the as-prepared FeOCl catalyst in 1.0 L of demineralized water with 10-min sonication. A cross-flow pre-filtration with the FeOCl suspension, spiked into the main feed stream (demineralized water), was then conducted to pre-coat a catalyst layer on the membrane surface in a filtration mode (Fig. S1, Supplementary Data). The pH value of the obtained FeOCl suspension was around 2.4, and was not further adjusted during the filtration-based pre-coating step. Herein, a laminar crossflow of 0.2 m s^{-1} (Reynolds number (Re) = 1510) and a high TMP (20.0 bar) were adopted to boost the formation and compaction of a uniform catalyst layer on the membrane surface. The resultant FeOCl pre-coated membranes were subjected to pure water filtration until the pH value of the permeate became the same as that of the feed pure water, in order to remove the acid and possible impurities from the FeOCl pre-coat layer. The influence of different FeOCl loading on permeance loss of the membrane was investigated by changing the FeOCl dosage in the feed flow from 6.2 to 13.2 and 23.1 mg L^{-1} during pre-coating. Thereafter, pure water permeance of the membrane before and after pre-coating was measured at TMP = 3.0 bar to determine the permeance loss.

2.3. Single- and multi-cycle fouling/cleaning experiments

Filtration experiments of pristine and FeOCl pre-coated membranes were performed in a constant-pressure mode with a bench-scale cross-flow filtration apparatus (OSMO Inspector 2, Convergence Industry, the Netherlands). High organic loading of sodium alginate (0.8 g L^{-1}) was adopted to develop accelerated fouling during a period of only 2 h, which simulates a five-day fouling period, obtained during pilot tests with ceramic NF of sewage [10]. NaCl (5.0 mM) and $CaCl_2$ (3.0 mM) were added as background salts to stimulate the formation of colloidal foulants, while $NaHCO_3$ (1.0 mM) was added as a buffer to maintain the solution at pH = 7.0. The filtration/cleaning protocol of the membranes comprised four sequential phases (Fig. 1a): (i) initial pure water flux (J_{w1}), (ii) flux decline (from J_{f1} to J_{f2}) during filtration with alginate solutions, (iii) membrane cleaning, and (iv) pure water flux (J_{w2}). The filtration and cleaning experiments were performed in duplicate, wherein the differences between the duplicate measurements of the membrane permeance before/during fouling and after cleaning were smaller than 5%. The concentrate was recirculated into the feed flow, while the permeate was consecutively collected for measuring the permeate flux over time, using a scale and a data acquisition system. The data acquisition system of the setup allowed to collect the flux data as a function of the filtration time every 1 min at least, because 1-min filtration was required for the membranes to collect a sufficient amount of permeate to reach the measurement limit of the scale. The temperature-corrected permeance was calculated according to Text S1 (Supplementary Data). Fouling characteristics and cleaning efficacy of the membranes were evaluated by calculating the initial fouling ratio (R_i), cake fouling ratio (R_c) and flux recovery ratio (F_r) with Eqs. (2)–(4), respectively.

$$R_i = \frac{J_{w1} - J_{f1}}{J_{w1}} \times 100\% \quad (2)$$

$$R_c = \frac{J_{f1} - J_{f2}}{J_{w1}} \times 100\% \quad (3)$$

$$F_r = \frac{J_{w2} - J_{f2}}{J_{w1} - J_{f2}} \times 100\% \quad (4)$$

2.3.1. Single cycle fouling

In order to explore the impact of different fouling characteristics of the membranes on the efficacy of Fenton cleaning, varying hydrodynamic conditions, i.e. TMP = 2.0, 3.0 and 4.0 bar and cross-flow velocity (CFV) = 0.3 and 0.9 m s^{-1}, were used in the single-cycle fouling experiments (1 h). Membrane cleaning experiments were executed by H_2O_2 circulation (30.0 or 60.0 mM, pH = 3.3) at a laminar cross flow (CFV = 0.2 m s^{-1}, Re = 1116) for 1 h (Fig. S1, Supplementary Data) to reduce hydraulic scouring over the pre-coat layer on the membrane. To compare with the efficacy of Fenton cleaning of the pre-coated membrane, a forward flush was conducted on the pristine membrane by circulating demineralized water inside the membrane channel at CFV = 2.2 m s^{-1} (Re = 15097) for 20 min without applying a TMP. To study the membrane fouling characteristics in the presence and absence of an FeOCl pre-coat layer, the same pristine membrane was used, first for the fouling test without pre-coating and then for the pre-coating/fouling test. Chemical cleaning by a sodium hypochlorite solution (0.2%) was performed between the two tests until reaching the initial permeance of the pristine membrane. To identify the cake fouling, variation of the filtered volume was described by the classical cake filtration law as presented in Eq. (5) [35,36]:

$$\frac{t}{V} = \frac{K_c}{2} V + \frac{1}{J_0} \quad (5)$$

where K_c (s m^{-2}) is the cake filtration constant, V (m^3) the filtered volume, J_0 the initial flux during filtration with the alginate solution, t the filtration time.

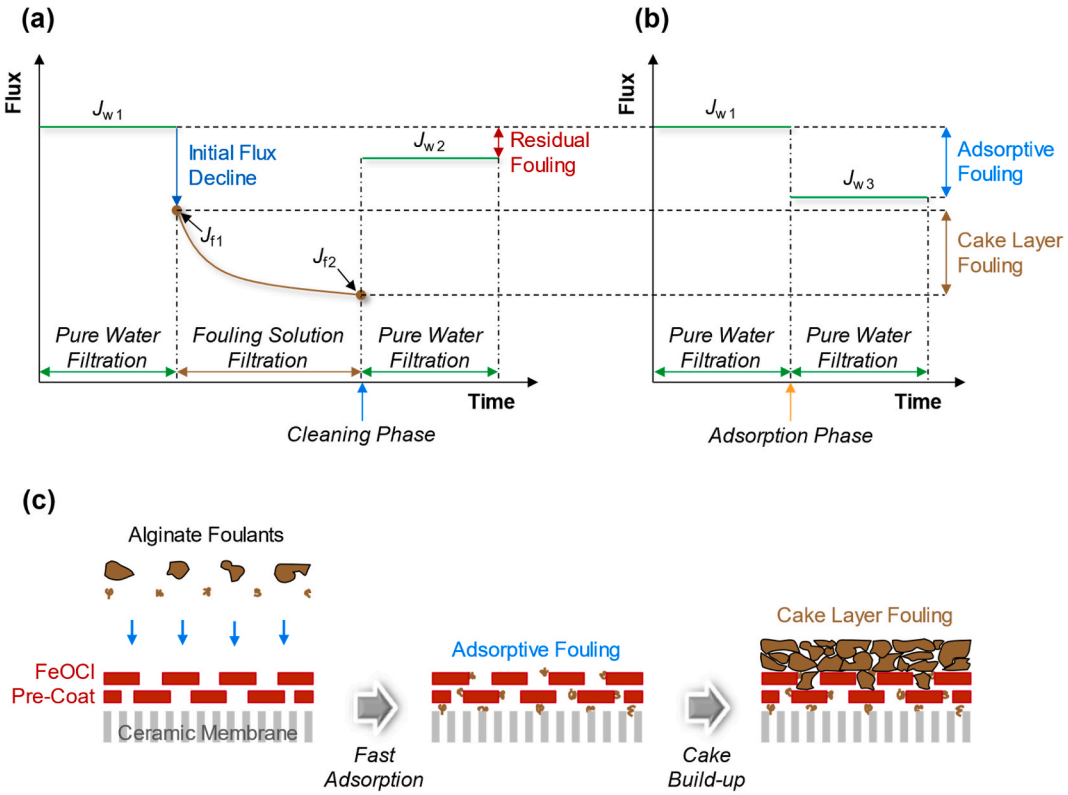

Fig. 1. Conceptual illustration of flux evolution over time of (a) fouling and (b) adsorption experiments. (c) Mechanistic illustration of assumed organic fouling steps during a filtration period with alginate solutions.

2.3.2. Multiple cycle fouling

The efficacy of Fenton cleaning of the FeOCl pre-coated membrane was further assessed over multiple cycles, using relatively thick and thin cake layer fouling, respectively, without renewing the pre-coat layer between the cycles to elucidate fouling/cleaning behaviour of the pre-coated membrane in repeated uses. The multiple-cycle fouling experiments were done with a turbulent flow (Re = 6039) inside the membrane channel at CFV = 0.9 m s^{-1}. The thick cake fouling was obtained during filtration with the alginate solution for 1 h at an initial pure water flux of 47.1 L m^{-2} h^{-1}. The thick cake fouling was cleaned by means of H_2O_2 flush ($[H_2O_2]_0$ = 60.0 mM, pH = 3.3), followed by forward flush with demineralized water, over three repeated cycles. The thin cake fouling was obtained during filtration with the alginate solution for 30 min (shorter than that for the thick cake fouling) at an initial pure water flux of 39.5 L m^{-2} h^{-1}, and cleaned by H_2O_2 flush ($[H_2O_2]_0$ = 30.0 mM, pH = 3.3), over five cycles. In order to study the relation between various fouling types (i.e. adsorptive fouling and cake growth) and Fenton cleaning, an adsorption step (5 min, as described in Section 2.4) was incorporated in the thick cake fouling test, prior to each cycle of filtration, using the same alginate solution. To further verify the effect of adsorptive fouling on Fenton cleaning, adsorption/cleaning was executed throughout five cycles, involving pure water filtration, adsorption with the alginate solution (30 min, the same as that for the thin cake fouling experiment) and Fenton cleaning ($[H_2O_2]_0$ = 30.0 mM, pH = 3.3) at each cycle, also without refreshing the pre-coat layer.

As the ceramic NF membranes were repeatedly used in the experiments after Fenton cleaning, potential defects of the membranes over the repeated uses were regularly measured by the method proposed by Kramer et al. [15] to ensure their right quality. The membranes did not show an increase in the percentage of their defects, which indicates a minor or no effect of Fenton cleaning on membrane aging.

2.4. Adsorption experiments of ceramic NF membranes

Adsorption of alginate foulants onto pristine and FeOCl pre-coated membranes was conducted in the same filtration apparatus and under the same crossflow conditions as were the fouling/cleaning experiments, only without a permeate flow (TMP = 0 bar) through the membranes. The adsorption experiments were to identify adsorptive fouling of the membranes and to distinguish its role in permeance decrease from that of cake fouling. As conceptually illustrated in Fig. 1b, the membranes were first subjected to filtration (TMP = 2.0 or 3.0 bar, CFV = 0.9 m s^{-1}) with demineralized water for 10 min to determine the initial pure water fluxes (denoted as J_{w1}). The initial pure water fluxes were used as a baseline to normalize the flux evolution before and after the adsorption steps. Prior to the start of adsorption, the demineralized water in the filtration setup was discharged and fully replaced with the alginate solution. Subsequently, the alginate solution was circulated within the membrane channel at CFV = 0.9 m s^{-1} for 1, 5 or 30 min, without allowing any permeate flow in the filtration system. Finally, demineralized water was filtered through the fouled membranes for 10 min to measure the pure water fluxes (denoted as J_{w3}) after adsorption. The adsorptive fouling ratios (R_a) were calculated, using Eq. (6), to assess the effect of foulant adsorption on initial flux declines.

$$R_a = \frac{J_{w1} - J_{w3}}{J_{w1}} \times 100\% \quad (6)$$

On the basis of the aforementioned adsorption and fouling experiments, a mechanistic explanation of the assumed organic fouling steps during a filtration period with the alginate solution is illustrated in Fig. 1c.

2.5. Characterization and analysis

Polyethylene glycols (PEGs) (Sigma-Aldrich, Germany) of five molecular weights (200, 300, 400, 600 and 1000 Da) were used as tracer compounds to determine the real molecular weight cut-off (MWCO) of the membrane, defined as the molecular weight of a tracer molecule that is retained with an efficiency of 90% by the membrane, as earlier reported by Shang et al. [37]. The PEG samples, collected in the feed and permeate solutions, were analysed by high-performance size exclusion chromatography (Prominence, Shimadzu, Japan), equipped with a refractive index detector (RID-20A, Shimadzu, Japan) and a gel permeation column (5 mm 30 Å, PSS GmbH, Germany). The particle size distribution of Ca-alginate colloids was measured with a blue laser diffraction particle size analyser (S3500, Microtrac Retsch GmbH, Germany). The top-view and cross-sectional images of the pristine and FeOCl pre-coated membranes were taken, using a scanning electron microscope (SEM) (S–3400 N, Hitachi High-Technologies, Japan) installed with energy dispersive spectroscopy. Atomic force microscopy (AFM) (Dimension FastScan, Bruker, USA) was used to measure average roughness (R_a) and root mean square roughness (R_q) of the membranes, which are defined as the arithmetic average of the profile height deviations from the mean plane, and the root mean square average of the profile height deviations from the mean plane, respectively.

3. Results and discussion

3.1. Characterization of membranes and foulants

A smooth and dense top surface was observed for the pristine membrane, without showing any visible defects on the membrane surface (Fig. 2a). The curve of PEG rejection as a function of PEG molecular weight (Fig. 2b) corresponds to a pore size of MWCO = 688 Da of the pristine membrane. Other studies have also reported larger actual MWCO values (450−1000 Da), as measured by crossflow filtration with an aqueous mixture of PEGs [9,38,39] or using a pore transport model with other reference organic tracers (i.e. xylose, dextrose and meso-erythritol) [40], than the nominal MWCO (200 or 450 Da, Inopor data) of similar membranes. As observed in Fig. 2c, the FeOCl particles on the membrane surface were present as long-strip sheets with, approximately, 4−6 μm in length, 1 μm in width and 0.2−0.3 μm in thickness, comparable to the dimensions of lab-prepared FeOCl reported elsewhere [28,41]. According to the AFM measurements (Fig. S2, Supplementary Data), the surface of the FeOCl pre-coated membrane (R_a = 21.67 nm and R_q = 28.97 nm) appeared to be rougher than that of the pristine membrane (R_a = 3.25 nm and R_q = 4.13 nm). The porous pre-coat layer, formed by stacking of the FeOCl particles on the membrane surface, had pore sizes of 0.1–0.5 μm, as estimated from Fig. 2c. As a result of the large pore sizes of the pre-coat layer relative to those (0.9 nm, Inopor data) of the separation layer, the pre-coat layer led to a minor reduction of 2.2–3.5% in the pure water permeance of the membrane, irrespective of the increase in the FeOCl loading from 0.29 to 0.94 g m^{-2} (Table S1, Supplementary Data). In other studies where particles (e.g. zirconium and iron oxides) were pre-coated on low-pressure membranes, however, a considerable decrease (>70%) in the pure water permeance occurred due to pore blockage, since the particle sizes and the pore sizes were similar [42,43]. As indicated by the cross-sectional SEM view and the corresponding Fe/Cl distribution on the pre-coated membrane (Fig. 2d), the pre-coat layer, having a thickness of around 4.6 μm, was uniformly coated on the membrane surface.

The colloids in the alginate solution had a particle size distribution of 10–1000 μm (Fig. S3, Supplementary Data), and were thus much larger than the pore sizes of the pre-coat layer. This implies that the Ca-alginate colloids, upon contact (or filtering) with the pre-coated membrane, would mostly deposit (or be intercepted) on the FeOCl pre-coat via steric exclusion, instead of directly contacting the separation layer [44]. The top-view SEM image of the pre-coated membrane after filtering the alginate solution (Fig. S4, Supplementary Data) shows a nearly complete covering of cake layer fouling on the pre-coat layer. However, apart from the large-sized alginate colloids, as suggested by Katsoufidou et al. [33] and Kim et al. [34], free alginate molecules are also expected to be

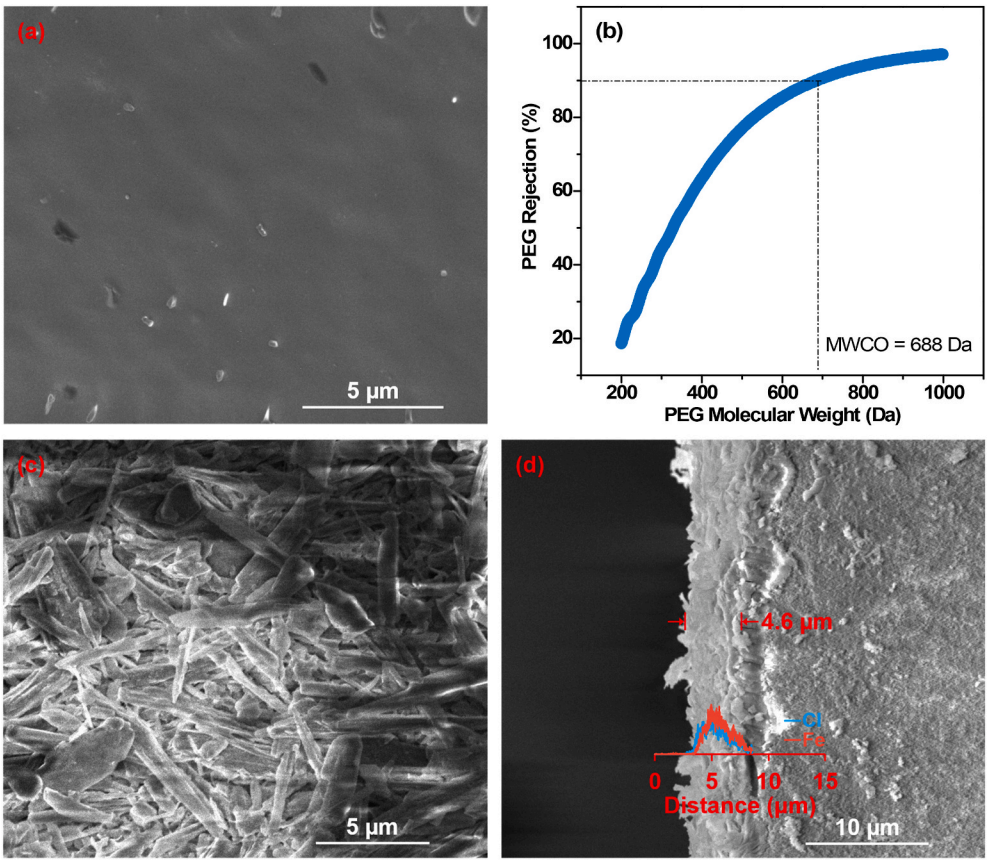

Fig. 2. (a) Top-view scanning electron microscope (SEM) image of pristine ceramic NF membrane. (b) Polyethylene glycol (PEG) rejection curve of the membrane. The dashed line shows the PEG molecular weight with a rejection rate of 90%. (c) Top-view and (d) cross-sectional SEM images with energy dispersive spectroscopy line scanning of Fe and Cl elements on the cross-section of FeOCl pre-coated membrane.

present in the solution, having a molecular weight distribution from 10 to >100 kDa, which means that the alginate molecules could penetrate the pre-coat layer and be adsorbed on/in the separation layer of the membrane.

3.2. Characteristics of flux decreases during alginate fouling

The pristine membrane first underwent an abrupt decline in the initial pure water flux, whereafter a gradual flux decrease followed (Fig. 3a), during filtration of the alginate solution. The time-dependent flux decreases during filtration with the alginate solution were in agreement with the linear relation of the cake filtration model (Section 2.3) with a correlation coefficient of $R^2 = 0.95–0.99$ (Fig. S5, Supplementary Data), thereby corresponding to the progressive build-up of a cake layer on the membrane [35,36]. Filtration at the high initial flux (64.0 L m^{-2} h^{-1}) developed a larger flux decline ($R_c = 39.5\%$) with the cake growth, than that ($R_c = 20.4\%$) at the lower initial flux (31.6 L m^{-2} h^{-1}), probably driven by the high permeate drag forces [45,46]. The cake fouling at the low initial flux was independent of the CFV, where 0.3 m s^{-1} corresponded to a laminar flow (Re = 2013.0) and 0.9 m s^{-1} to a turbulent flow (Re = 6038.9), respectively. It is thus suggested that the alginate cake layer had a high adhesion affinity towards the pristine membrane and was thus able to resist the crossflow shear forces, presumably resulting from the formation of aggregates with low back diffusion [47]. Herein, the applied TMPs (2–4 bar) were lower than those in ceramic NF-based wastewater treatment applications (4–16 bar) [6,7], but the permeate fluxes (13–44 L m^{-2} h^{-1}), obtained in the fouling experiments, were regular for ceramic NF processes. As an example, Cabrera et al. reported that direct ceramic NF with industrial wastewater at TMP = 4–16 bar generated a permeate flux of about 20–30 L m^{-2} h^{-1} [7], comparable to the fluxes in our experiments.

As depicted in Fig. 3b, the initial pure water permeabilities at both TMP = 2.0 and 4.0 bar were similar, while, during filtration with the alginate solution, the permeability decreased to a lower level (4.2 L m^{-2} h^{-1} bar^{-1}) at TMP = 4.0 bar compared to TMP = 2.0 bar (6.5 L m^{-2} h^{-1} bar^{-1}). This is likely a result of the formation of a thicker, more compact cake layer at the higher flux, since more foulants could be transported to the membrane surface as a result of the faster cake build-up [48]. This observation is not in line with the findings of Akamatsu et al., who demonstrated an unchanged filtration resistance with an increase in permeate flux, during NF of a sole alginate solution, probably due to the lower compressibility of the long-chain alginate molecules they used, while here the coiled Ca-alginate colloids were filtered [49].

Fig. 3c displays the flux profiles of the pristine and FeOCl pre-coated membranes operated under initial fluxes of 56.7 and 46.2 L m^{-2} h^{-1}, respectively. The same membrane was used for these comparative experiments (see Section 2.3). The pristine and pre-coated membranes developed a sharp decline in the individual pure water flux, after pre-adsorption (5 min), and a progressive flux decrease, during filtration with the alginate solution. Moreover, as illustrated in Fig. 3d, good linear fits ($y = 0.99\,x + 6.36$ and $y = 1.05\,x + 6.54$, $R^2 = 0.99$) to the cake filtration model were observed for the progressive flux decreases of both membranes. The results indicate that the two stages of the flux reductions were attributed to an abrupt transition of the fouling mechanism from initial rapid adsorption of the foulants to subsequent gradual cake growth on the membranes, thereby verifying the proposed mechanistic explanation about the underlying fouling steps of the membranes during a filtration period with the alginate solution (Fig. 1c). In addition, the fouling characteristics during cake build-up were independent of the presence of the pre-coat layer, as suggested by the nearly same flux

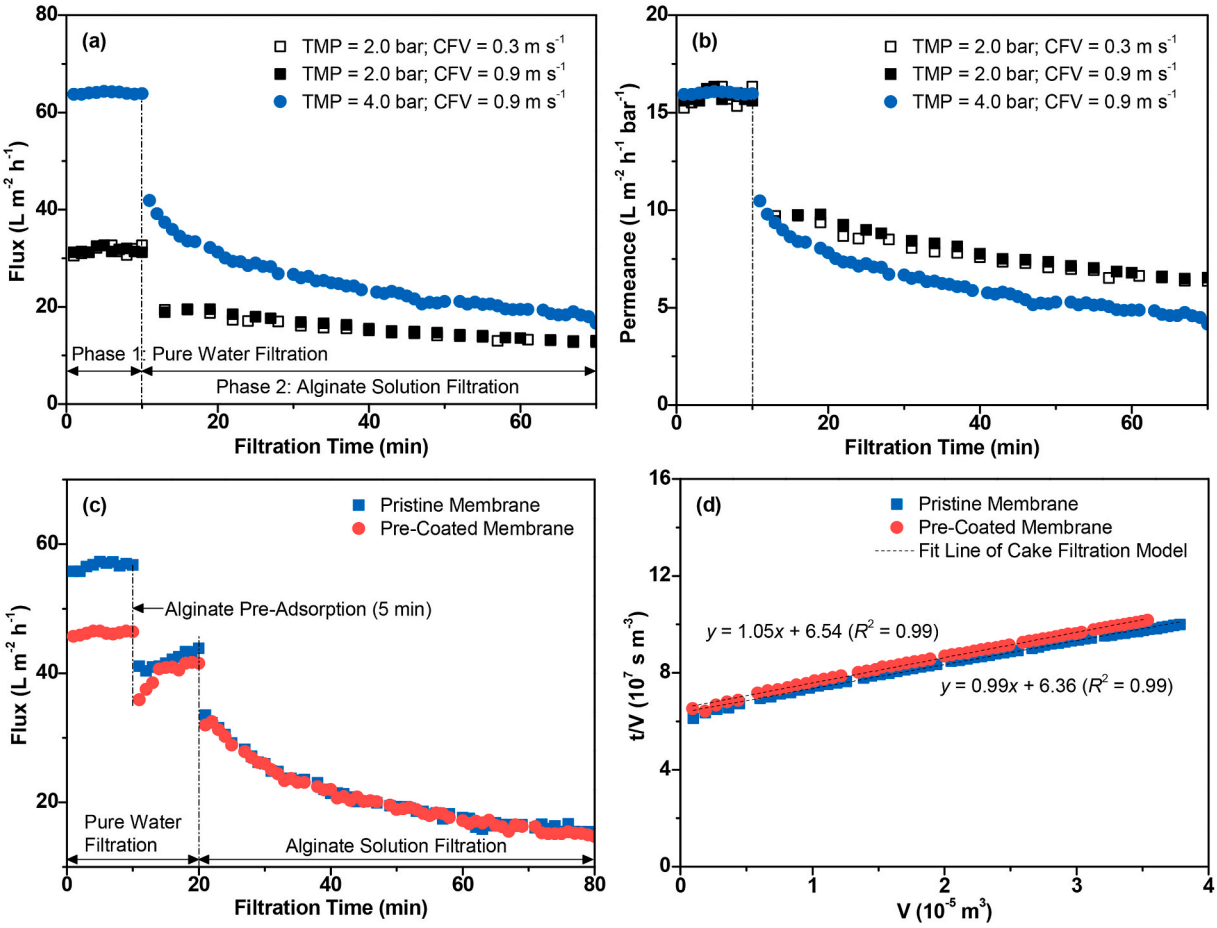

Fig. 3. Variations in (a) water flux and (b) membrane permeance during filtration under different transmembrane pressures (TMPs) and cross-flow velocities (CFVs) with pristine ceramic NF membrane. (c) Flux evolution and (d) t/V vs. V variation profiles of pristine and FeOCl pre-coated membranes operated at TMP = 3.0 bar and CFV = 0.9 m s^{-1}. The straight lines correspond to the linear fitting of t/V vs. V profiles to the cake filtration model.

decline curves of the two membranes (Fig. 3c), which is in agreement with previous studies regarding other pre-coat types (e.g. floc/particulate $FeCl_3$ and Fe_3O_4 layers) [13,25]. It is thus expected that the FeOCl pre-coat layer was not compressed during fouling, since a sufficiently compact structure of the pre-coat layer could have been formed during pre-coating under a high TMP (20.0 bar, Section 2.2).

3.3. Adsorptive fouling as a mechanism for initial rapid flux decline

For evaluating the rate of rapid fouling at the start of a filtration cycle, the decline of initial pure water fluxes, caused by membrane fouling in the absence of a permeate flow, was separated from the subsequent gradual flux decrease due to cake build-up. Short contact periods, i.e. 1 and 5 min, were adopted in the adsorption tests, to simulate the early stage of fouling resulting from foulant adsorption. Fig. 4 depicts the variations of the pure water fluxes over the pristine and FeOCl pre-coated membranes, upon exposure to the alginate solution. The pristine membrane, after 5 min contact with the alginate solution without a permeate flow, displayed a pure water flux reduction of 32.5%, while adsorptive fouling was considered to be the only cause for the flux decline, since no cake layer was able to build up in the absence of a permeate flow [45,49]. The adsorption test with a shorter contact time of 1 min caused a flux decline of 25.9%, which suggests that adsorption of the foulants onto the pristine membrane rapidly took place. However, the FeOCl pre-coated membrane, upon exposure to the alginate solution, within the same time frame (5 min), underwent a smaller decline (14.5%) in the pure water flux compared to the pristine membrane. This is presumably due to the adsorption of foulants on the

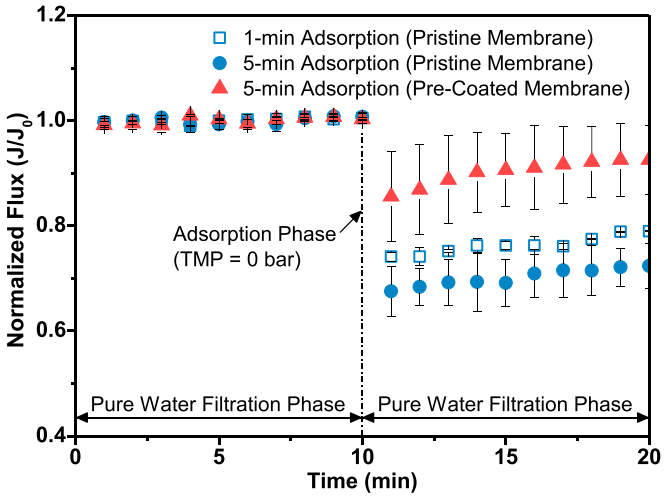

Fig. 4. Experimental determination of permeance declines due to foulant adsorption onto pristine and FeOCl pre-coated membranes at pH = 7.0. The duration of the pure water filtration phase before adsorption, adsorption phase and pure water filtration phase after adsorption was 10, 1 (or 5) and 10 min, respectively.

pre-coat layer without adding to the flux decline, as a result of the large pore sizes of the pre-coat layer. Similar findings have previously been reported for other types of pre-coat layers (e.g. iron oxide and

aluminium oxide layers) on ceramic membranes, acting as a pre-filtration media for organic molecules and colloids prior to reaching the separation layers of the membranes [44,50].

Additionally, both membranes developed, during the adsorption experiments, a gradual increase in their fluxes during filtration with pure water after the adsorption phases. This result indicates that the adsorbed foulants could be, to some extent, desorbed from the membranes along with the crossflow filtration processes, supposedly due to hydraulic scouring. As also observed in Fig. 3c, however, the progressive increases in the pure water fluxes after pre-adsorption do not mean that the membranes would suffer less adsorptive fouling at the beginning of the alginate filtration phase, since new adsorptive fouling could occur on/in the membranes upon contact with the alginate solution.

3.4. Dependence of cleaning efficacy on fouling characteristics during a single fouling cycle

Fenton cleaning was based on the activation of Fenton reactions on the FeOCl pre-coated membrane, using the FeOCl pre-coat layer as the catalyst and a H_2O_2 solution as the key Fenton reagent. $^{\bullet}OH$ radicals, as the main reactive oxygen species for oxidizing the organic foulants, could be generated by H_2O_2 decomposition at the catalytic sites of the FeOCl particles through the Fenton reactions as indicated in Eq. (7) and Eq. (8) [26,27,51].

$$FeOCl + H_2O_2 \leftrightarrow Fe^{III}_{1-n}Fe^{II}_{n} + {}^{\bullet}OOH + H^{+} \quad (7)$$

$$\equiv Fe^{II} + H_2O_2 \leftrightarrow \equiv Fe^{III} + {}^{\bullet}OH + OH^{-} \quad (8)$$

As suggested in several studies, a fouling layer on catalytic membranes is likely to behave as a barrier for the diffusion of H_2O_2 onto the active sites, thereby hampering the Fenton oxidation of organic foulants [16,17]. Therefore, in the present study, the efficacy of Fenton cleaning for the FeOCl pre-coated membrane, was assessed for both thin and thick cake fouling, in comparison with using demineralized water forward flush and sole H_2O_2 cleaning of the pristine membrane (Fig. 5a and b). The thin cake fouling of the membranes was obtained by starting fouling at a comparatively low initial flux (29.3–40.5 L m^{-2} h^{-1}) for 30 min, while for the thick cake fouling an initial flux of 46.3–57.2 L m^{-2} h^{-1} for 60 min, corresponding to cake fouling ratios of R_c = 11.5–17.0% and 34.5–35.6%, respectively (Fig. 5a). As depicted in Fig. 5b, forward flush of the pristine membrane slightly recovered the pure water flux, by 17.5% and 15.9%, at the thin and thick cake fouling conditions, respectively, indicating that the majority of the alginate foulants were strongly attached to the membrane surface and could resist hydraulic scouring [12,13]. H_2O_2 flush ($[H_2O_2]_0$ = 30.0 mM) of the pristine membrane seemed effective in pure water flux restoration (F_r = 67.6%) for the thin cake fouling, but less effective (F_r = 14.4%) for the thick cake fouling, even at a high dosage of H_2O_2 ($[H_2O_2]_0$ = 60.0 mM). H_2O_2 cleaning in the presence of an FeOCl pre-coat layer on the membrane, increased the flux recovery to 98.5% for the thin cake fouling, suggesting effective Fenton oxidation during crossflow flush with the H_2O_2 solution. Hence, the adsorptive fouling and the deposited cake layer on/in the FeOCl pre-coat, tended to be degraded by the generated $^{\bullet}OH$ radicals. However, a lower flux recovery of 65.4% was obtained after Fenton cleaning ($[H_2O_2]_0$ = 60 mM) of the thick cake fouling. The dependence of the Fenton cleaning efficacy on the fouling characteristics, could be ascribed to increased deposition and compacted conformation of cake layers as a result of high-flux convection (as described in Section 3.2), which could slow down the diffusion of H_2O_2 through the cake layer into the FeOCl pre-coat [52–54].

3.5. Fenton cleaning in relation to fouling types over multiple cycles

3.5.1. Cleaning of cake layer dominated fouling

To study the efficacy of Fenton cleaning in relation to the type of fouling on the FeOCl pre-coated membrane, combined pre-adsorption/cake filtration/cleaning steps were sequentially executed over three cycles without refreshing the pre-coat layer. The experiment was performed using an initial flux of 47.1 L m^{-2} h^{-1}, corresponding to the relatively thick cake layer fouling as discussed in Section 3.4. As presented in Fig. 6, a sharp flux decline, due to initial fast adsorption of the foulants, and a progressive flux decrease, resulting from subsequent cake build-up, were separately observed at each cycle of adsorption and filtration with the alginate solution. Upon combined Fenton cleaning/forward flush after *Cycle 1* and *2*, the initial pure water fluxes at *Cycle 2* and *3* were recovered to J/J_0 = 78.0% and 82.5%, respectively, which represent the cleaning efficacy of the total fouling (i.e. adsorptive and cake fouling) at each cycle. In the meantime, however, the average fluxes during cake filtration at *Cycle 2* and *3* were restored to a larger extent, i.e. by 92.1% and 92.3% (relative to the average cake filtration flux at *Cycle 1*), respectively, corresponding to the cleaning efficacy of the cake layer fouling. The results indicate that the cake layer fouling of the pre-coated membrane was much better cleaned than was the adsorptive fouling. This is presumably because the cake layer fouling occurred on the surface of the pre-coated membrane where the reactive FeOCl catalyst was present, while the adsorptive fouling was situated in the pores of the TiO_2 separation layer without the presence of the catalyst. Therefore, the characteristics (e.g. thickness) of the separation

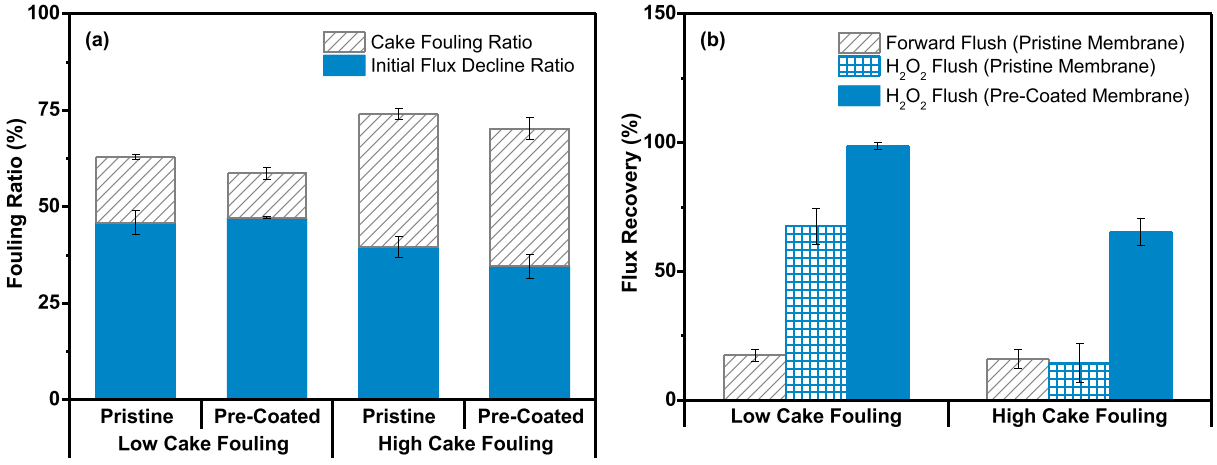

Fig. 5. (a) Initial flux decline ratios and cake fouling ratios during thin cake fouling (J_0 = 29.3–40.5 L m^{-2} h^{-1}, fouling duration = 30 min) and during thick cake fouling (J_0 = 46.3–57.2 L m^{-2} h^{-1}, fouling duration = 60 min), respectively, using pristine and FeOCl pre-coated membranes. (b) Cleaning efficiencies of forward flush with demineralized water or H_2O_2 solutions (pH = 3.3) during a single fouling cycle of the membranes.

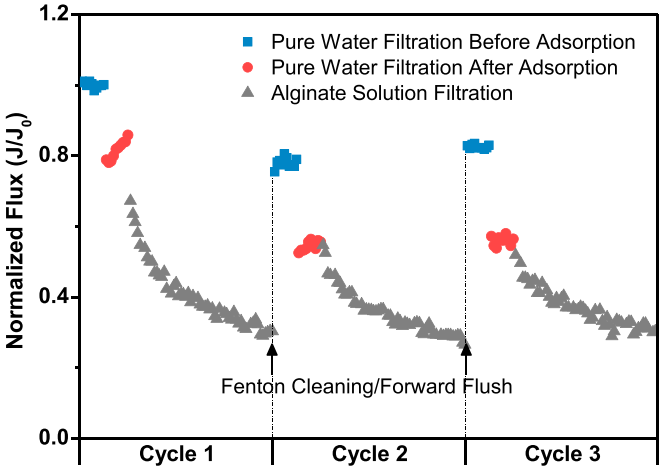

Fig. 6. Multiple cycles of pure water filtration (J_0 = 47.1 L m^{-2} h^{-1}) and combined pre-adsorption/filtration with an alginate solution using an FeOCl pre-coated membrane, with periodical Fenton cleaning ([H_2O_2]$_0$ = 60.0 mM, pH = 3.3) followed by demineralized water forward flush.

layer are expected to only affect the adsorptive fouling, which might increase with an increase in thickness of the separation layer. The cake layer fouling, however, would not be influenced by the thickness of the separation layer, because this type of fouling was only located on top of the separation layer with constant compression during constant pressure filtration.

Nonetheless, the removal of the adsorptive fouling seemed to be less important than that of the cake layer fouling, since new adsorptive fouling rapidly occurred on/in the cleaned membrane upon contact with the alginate solution at *Cycle 2* and *3*, as indicated by the abrupt pure water flux declines of 25.5% and 25.3%, respectively. The actual water production capacity during ceramic NF over the multiple cycles was predominantly determined by the fluxes during cake filtration, because the adsorptive fouling only occurred at the very beginning of each filtration cycle. Similar observations have also been reported for other type of oxidative cleaning, such as chlorine cleaning [55].

3.5.2. *Cleaning of adsorption dominated fouling*

To further explore the efficacy of Fenton cleaning on adsorptive fouling, interference of cake fouling accumulation over multiple cycles should be excluded. For this purpose, a multiple-cycle filtration/cleaning experiment was done with adsorption-dominated fouling (i.e. thin cake layer fouling, as described in Section 3.4), obtained by filtration at an initial flux of 39.5 L m^{-2} h^{-1} for a short period (30 min) at each cycle, in parallel to a multiple-cycle adsorption/cleaning experiment (see Section 2.3). As depicted in Fig. 7a, the initial sharp flux declines (R_i = 43.9–46.8%), occurring as a result of rapid adsorption at the very beginning of filtration with the alginate solution, predominantly accounted for the total flux decrease ($R_i + R_c$ = 56.0–58.1%) at each cycle, which confirms the dominance of adsorptive fouling in this experiment. The pure water flux gradually decreased over the five filtration/cleaning cycles, in particular, at *Cycle 4* and *5* (dropping to J/J_0 = 0.91 and 0.87, respectively), while the fluxes during the multiple cake filtration periods remained similar in the range of J/J_0 = 0.42–0.55, approximately. This result suggests that the cake layer fouling formed at each cycle was entirely removed by Fenton cleaning, whilst some adsorptive fouling progressively accumulated on/within the separation layer of the membrane at the later cycles. However, the remaining adsorptive fouling after Fenton cleaning did not influence the total permeate production, as the fluxes during cake filtration were unchanged over the five cycles.

The multiple-cycle adsorption/cleaning experiment was performed under the same conditions as the multiple-cycle filtration/cleaning test, without allowing a permeate flow during adsorption. As shown in Fig. 7b, the pure water fluxes after periodical Fenton cleaning followed a descending trend from J/J_0 = 1 to 0.93, confirming that a proportion of the adsorbed foulants were not reversed by the cleaning steps and tended to accumulate on/in the separation layer of the membrane. This observation is in agreement with the decreasing trend of the pure water flux in the multiple-cycle filtration/cleaning experiment (Fig. 7a), which thus verifies that the gradual flux decrease over the multiple filtration/cleaning cycles was mainly attributed to progressive accumulation of the remaining adsorptive fouling. Nonetheless, the pure water fluxes after multiple-cycle adsorption remained stable, in the range of J/J_0 = 0.68–0.72, from *Cycle 1* to *5*, implying that the total amount of the remaining and new adsorptive fouling on/within the separation layer of the membrane at each cycle was independent of the progressive accumulation of the remaining adsorptive fouling. It is likely that the limited number of adsorption sites on/in the separation layer of the membrane corresponded to the constant amount of the total adsorptive fouling (consisting of the remaining and new adsorptive fouling) during the multiple adsorption/cleaning cycles [56]. The results confirm the aforementioned minimal impact of the incomplete removal (or gradual accumulation) of the remaining adsorptive fouling on the flux evolution during cake filtration, i.e. the total permeate production, using pre-coated ceramic NF in combination with Fenton cleaning.

3.6. *Research needs and challenges*

The initial adsorption of the foulants occurred within 1 min, while

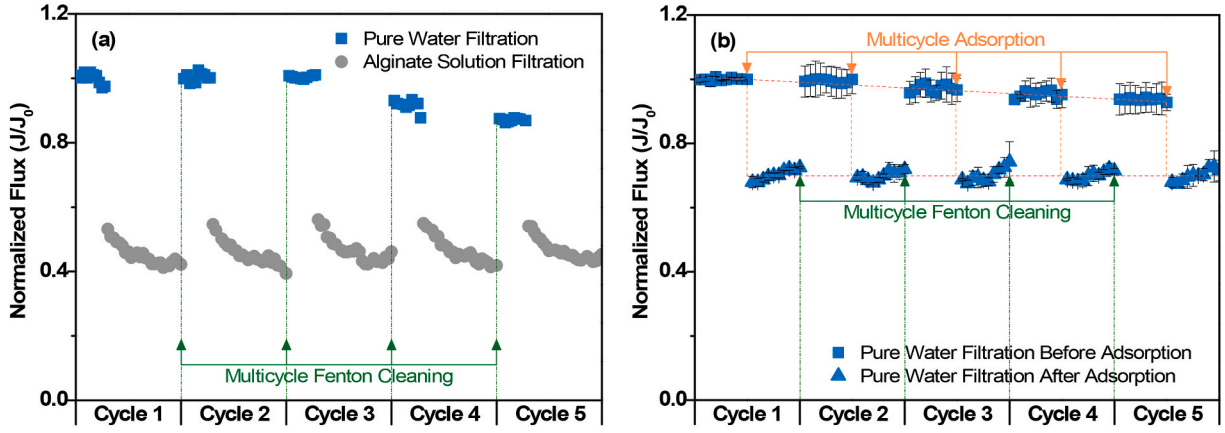

Fig. 7. Multiple-cycle (a) filtration (J_0 = 39.5 L m^{-2} h^{-1}) and (b) adsorption with alginate solutions and periodical Fenton cleaning ([H_2O_2]$_0$ = 30.0 mM, pH = 3.3) using an FeOCl pre-coated membrane.

the data acquisition system of our experiments was only able to collect the flux data every 1 min at least. Therefore, the initial rapid adsorption behaviour of the ceramic NF membranes was not fully recorded and still needs to be further studied by, e.g., using more continuous data acquisition and proper model fitting.

In this study, we only performed the five cycles (30 or 60 min for each cycle) of filtration with the concentrated alginate feed water to simulate a long-term filtration operation (up to 12.5 d) with real wastewater. Therefore, pilot ceramic NF research on a longer-period scale, using real wastewater in combination with Fenton cleaning, is needed for further validation of the practicability of the concepts behind this work.

4. Conclusions

A better understanding of the relation between oxidative cleaning efficacy and fouling characteristics is of practical significance for ceramic membrane-based wastewater reclamation in combination with oxidative cleaning regimes. In this study, the efficacy of Fenton cleaning of an FeOCl pre-coated ceramic NF membrane was assessed in relation to its different fouling types under a high organic loading condition. For this purpose, membrane adsorption and constant-pressure filtration experiments with synthetic wastewater (i.e. a highly concentrated alginate solution in the presence of calcium ions) were performed in parallel, to differentiate between permeance decreases as a result of adsorptive fouling and cake layer fouling, respectively.

The results demonstrate that the flux evolution could be divided into an initial sharp flux decline, due to fast adsorption of the foulants (i.e. adsorptive fouling), and a subsequent gradual flux decline, resulting from progressive cake build-up on the membrane (i.e. cake layer fouling). During fouling and Fenton cleaning of the FeOCl pre-coated membrane over multiple cycles, Fenton cleaning was able to sufficiently remove the cake layer fouling in contrast to the adsorptive fouling. However, the total permeate production during ceramic NF was not influenced by the remaining adsorptive fouling (after Fenton cleaning). This is because the total amount of the adsorptive fouling, consisting of the remaining adsorptive fouling after each cleaning cycle and the new adsorptive fouling occurring at the very beginning of each filtration cycle, was constant presumably due to the limited number of adsorption sites on/in the membrane. Therefore, the removal of the adsorptive fouling during ceramic NF was of minor importance for the overall performance in water production.

Author statement

Bin Lin: Conceptualization, Methodology, Investigation, Data curation, Writing - original draft.

Luuk C. Rietveld: Writing - review & editing, Supervision.

Lu Yao: Investigation, Data curation.

Sebastiaan G.J. Heijman: Conceptualization, Methodology, Writing - review & editing, Supervision.

Declaration of competing interest

The authors declare that they have no known competing financial interests or personal relationships that could have appeared to influence the work reported in this paper.

Data availability

Data will be made available on request.

Acknowledgement

The authors acknowledge the PhD scholarship awarded to Bin Lin (No. 201706190224) by the China Scholarship Council, China.

Appendix A. Supplementary data

Supplementary data to this article can be found online at https://doi.org/10.1016/j.memsci.2023.122097.

References

[1] C. Boo, Y. Wang, I. Zucker, Y. Choo, C.O. Osuji, M. Elimelech, High performance nanofiltration membrane for effective removal of perfluoroalkyl substances at high water recovery, Environ. Sci. Technol. 52 (2018) 7279–7288, https://doi.org/10.1021/acs.est.8b01040.

[2] W.J. Lau, A.F. Ismail, Polymeric nanofiltration membranes for textile dye wastewater treatment: preparation, performance evaluation, transport modelling, and fouling control — a review, Desalination 245 (2009) 321–348, https://doi.org/10.1016/j.desal.2007.12.058.

[3] A.I. Radu, M.S.H. van Steen, J.S. Vrouwenvelder, M.C.M. van Loosdrecht, C. Picioreanu, Spacer geometry and particle deposition in spiral wound membrane feed channels, Water Res. 64 (2014) 160–176, https://doi.org/10.1016/j.watres.2014.06.040.

[4] U.K. Rai, M. Muthukrishnan, B.K. Guha, Tertiary treatment of distillery wastewater by nanofiltration, Desalination 230 (2008) 70–78, https://doi.org/10.1016/j.desal.2007.11.017.

[5] M.T.T. Ngo, T. Ueyama, R. Makabe, X.T. Bui, L.D. Nghiem, T.T.V. Nga, T. Fujioka, Fouling behavior and performance of a submerged flat-sheet nanofiltration membrane system for direct treatment of secondary wastewater effluent, J. Water Process Eng. 41 (2021), 101991, https://doi.org/10.1016/j.jwpe.2021.101991.

[6] S. Motta Cabrera, L. Winnubst, H. Richter, I. Voigt, A. Nijmeijer, Industrial application of ceramic nanofiltration membranes for water treatment in oil sands mines, Sep. Purif. Technol. 256 (2021), 117821, https://doi.org/10.1016/j.seppur.2020.117821.

[7] S.M. Cabrera, L. Winnubst, H. Richter, I. Voigt, J. McCutcheon, A. Nijmeijer, Performance evaluation of an industrial ceramic nanofiltration unit for wastewater treatment in oil production, Water Res. 220 (2022), 118593, https://doi.org/10.1016/j.watres.2022.118593.

[8] Y. Lee, M. Cha, Y. So, I.H. Song, C. Park, Functionalized boron nitride ceramic nanofiltration membranes for semiconductor wastewater treatment, Sep. Purif. Technol. 300 (2022), 121945, https://doi.org/10.1016/j.seppur.2022.121945.

[9] G. Mustafa, K. Wyns, A. Buekenhoudt, V. Meynen, Antifouling grafting of ceramic membranes validated in a variety of challenging wastewaters, Water Res. 104 (2016) 242–253, https://doi.org/10.1016/j.watres.2016.07.057.

[10] F.C. Kramer, R. Shang, S.G.J. Heijman, S.M. Scherrenberg, J.B. van Lier, L. C. Rietveld, Direct water reclamation from sewage using ceramic tight ultra- and nanofiltration, Sep. Purif. Technol. 147 (2015) 329–336, https://doi.org/10.1016/j.seppur.2015.04.008.

[11] T. Fujioka, A.T. Hoang, T. Okuda, H. Takeuchi, H. Tanaka, L.D. Nghiem, Water reclamation using a ceramic nanofiltration membrane and surface flushing with ozonated water, Int. J. Environ. Res. Publ. Health 15 (2018) 799, https://doi.org/10.3390/ijerph15040799.

[12] Y.Y. Zhao, X.M. Wang, H.W. Yang, Y.F. Xie, Effects of organic fouling and cleaning on the retention of pharmaceutically active compounds by ceramic nanofiltration membranes, J. Membr. Sci. 563 (2018) 734–742, https://doi.org/10.1016/j.memsci.2018.06.047.

[13] F.C. Kramer, R. Shang, L.C. Rietveld, S.J.G. Heijman, Fouling control in ceramic nanofiltration membranes during municipal sewage treatment, Sep. Purif. Technol. 237 (2020), 116373, https://doi.org/10.1016/j.seppur.2019.116373.

[14] S.S. Wadekar, R.D. Vidic, Comparison of ceramic and polymeric nanofiltration membranes for treatment of abandoned coal mine drainage, Desalination 440 (2018) 135–145, https://doi.org/10.1016/j.desal.2018.01.008.

[15] F.C. Kramer, R. Shang, S.M. Scherrenberg, L.C. Rietveld, S.J.G. Heijman, Quantifying defects in ceramic tight ultra- and nanofiltration membranes and investigating their robustness, Sep. Purif. Technol. 219 (2019) 159–168, https://doi.org/10.1016/j.seppur.2019.03.019.

[16] S. Sun, H. Yao, W. Fu, L. Hua, G. Zhang, W. Zhang, Reactive Photo-Fenton ceramic membranes: synthesis, characterization and antifouling performance, Water Res. 144 (2018) 690–698, https://doi.org/10.1016/j.watres.2018.08.002.

[17] L. De Angelis, M.M.F. de Cortalezzi, Improved membrane flux recovery by Fenton-type reactions, J. Membr. Sci. 500 (2016) 255–264, https://doi.org/10.1016/j.memsci.2015.11.042.

[18] Y. Zhu, S. Chen, X. Quan, Y. Zhang, C. Gao, Y. Feng, Hierarchical porous ceramic membrane with energetic ozonation capability for enhancing water treatment, J. Membr. Sci. 431 (2013) 197–204, https://doi.org/10.1016/j.memsci.2012.12.048.

[19] H. Park, Y. Kim, B. An, H. Choi, Characterization of natural organic matter treated by iron oxide nanoparticle incorporated ceramic membrane-ozonation process, Water Res. 46 (2012) 5861–5870, https://doi.org/10.1016/j.watres.2012.07.039.

[20] X. Wang, Y. Li, H. Yu, F. Yang, C.Y. Tang, X. Quan, Y. Dong, High-flux robust ceramic membranes functionally decorated with nano-catalyst for emerging micro-pollutant removal from water, J. Membr. Sci. 611 (2020), 118281, https://doi.org/10.1016/j.memsci.2020.118281.

[21] Y. Bao, W.J. Lee, T.T. Lim, R. Wang, X. Hu, Pore-functionalized ceramic membrane with isotropically impregnated cobalt oxide for sulfamethoxazole degradation and membrane fouling elimination: synergistic effect between catalytic oxidation and membrane separation, Appl. Catal. B Environ. 254 (2019) 37–46, https://doi.org/10.1016/j.apcatb.2019.04.081.

[22] L. Zhu, W. Wang, P. Zhao, S. Wang, K. Yang, H. Shi, M. Xu, Y. Dong, Silicon carbide catalytic ceramic membranes with nano-wire structure for enhanced anti-fouling performance, Water Res. 226 (2022), 119209, https://doi.org/10.1016/j.watres.2022.119209.
[23] S. Zhang, L. Gutierrez, F. Qi, J.P. Croue, $SO4^{\bullet-}$-based catalytic ceramic UF membrane for organics removal and flux restoration, Chem. Eng. J. 398 (2020), 125600, https://doi.org/10.1016/j.cej.2020.125600.
[24] G. Mustafa, K. Wyns, P. Vandezande, A. Buekenhoudt, V. Meynen, Novel grafting method efficiently decreases irreversible fouling of ceramic nanofiltration membranes, J. Membr. Sci. 470 (2014) 369–377, https://doi.org/10.1016/j.memsci.2014.07.050.
[25] B. Lin, S.G.J. Heijman, R. Shang, L.C. Rietveld, Integration of oxalic acid chelation and Fenton process for synergistic relaxation-oxidation of persistent gel-like fouling of ceramic nanofiltration membranes, J. Membr. Sci. 636 (2021), 119553, https://doi.org/10.1016/j.memsci.2021.119553.
[26] M. Sun, I. Zucker, D.M. Davenport, X. Zhou, J. Qu, M. Elimelech, Reactive, self-cleaning ultrafiltration membrane functionalized with iron oxychloride nanocatalysts, Environ. Sci. Technol. 52 (2018) 8674–8683, https://doi.org/10.1021/acs.est.8b01916.
[27] X.J. Yang, X.M. Xu, J. Xu, Y.F. Han, Iron oxychloride (FeOCl): an efficient Fenton-like catalyst for producing hydroxyl radicals in degradation of organic contaminants, J. Am. Chem. Soc. 135 (2013), https://doi.org/10.1021/ja409130c, 16058−16061.
[28] M. Sun, C. Chu, F. Geng, X. Lu, J. Qu, J. Crittenden, M. Elimelech, J.H. Kim, Reinventing Fenton chemistry: iron oxychloride nanosheet for pH-insensitive H_2O_2 activation, Environ. Sci. Technol. Lett. 5 (2018) 186–191, https://doi.org/10.1021/acs.estlett.8b00065.
[29] S. Meng, R. Wang, X. Meng, Y. Wang, W. Fan, D. Liang, M. Zhang, Y. Liao, C. Tang, Reaction heterogeneity in the bridging effect of divalent cations on polysaccharide fouling, J. Membr. Sci. 641 (2022), 119933, https://doi.org/10.1016/j.memsci.2021.119933.
[30] Y. Wang, X. Zheng, Z. Wang, Z. Shi, Z. Kong, M. Zhong, J. Xue, Y. Zhang, Effects of –COOH and $–NH_2$ on adsorptive polysaccharide fouling under varying pH conditions: contributing factors and underlying mechanisms, J. Membr. Sci. 621 (2021), 118933, https://doi.org/10.1016/j.memsci.2020.118933.
[31] Y. Guo, T.Y. Li, K. Xiao, X.M. Wang, Y.F. Xie, Key foulants and their interactive effect in organic fouling of nanofiltration membranes, J. Membr. Sci. 610 (2020), 118252, https://doi.org/10.1016/j.memsci.2020.118252.
[32] L. De Angelis, M.M.F. de Cortalezzi, Ceramic membrane filtration of organic compounds: effect of concentration, pH, and mixtures interactions on fouling, Sep. Purif. Technol. 118 (2013) 762–775, https://doi.org/10.1016/j.seppur.2013.08.016.
[33] K. Katsoufidou, S.G. Yiantsios, A.J. Karabelas, Experimental study of ultrafiltration membrane fouling by sodium alginate and flux recovery by backwashing, J. Membr. Sci. 300 (2007) 137–146, https://doi.org/10.1016/j.memsci.2007.05.017.
[34] H.C. Kim, B.A. Dempsey, Membrane fouling due to alginate, SMP, EfOM, humic acid, and NOM, J. Membr. Sci. 428 (2013) 190–197, https://doi.org/10.1016/j.memsci.2012.11.004.
[35] W. Yao, Z. Wang, P. Song, The cake layer formation in the early stage of filtration in MBR: mechanism and model, J. Membr. Sci. 559 (2018) 75–86, https://doi.org/10.1016/j.memsci.2018.04.042.
[36] S. Ognier, C. Wisniewski, A. Grasmick, Influence of macromolecule adsorption during filtration of a membrane bioreactor mixed liquor suspension, J. Membr. Sci. 209 (2002) 27–37, https://doi.org/10.1016/S0376-7388(02)00123-0.
[37] R. Shang, A. Goulas, C.Y. Tang, X. de Frias Serra, L.C. Rietveld, S.G.J. Heijman, Atmospheric pressure atomic layer deposition for tight ceramic nanofiltration membranes: synthesis and application in water purification, J. Membr. Sci. 528 (2017) 163–170, https://doi.org/10.1016/j.memsci.2017.01.023.
[38] I. Caltran, L.C. Rietveld, H.L. Shorney-Darby, S.G.J. Heijman, Separating NOM from salts in ion exchange brine with ceramic nanofiltration, Water Res. 179 (2020), 115894, https://doi.org/10.1016/j.watres.2020.115894.
[39] Y. So, Y. Lee, S. Kim, J. Lee, C. Park, Role of co-existing ions in the removal of dissolved silica by ceramic nanofiltration membrane, J. Water Process Eng. 53 (2023), 103873, https://doi.org/10.1016/j.jwpe.2023.103873.
[40] M. Cha, C. Boo, C. Park, Simultaneous retention of organic and inorganic contaminants by a ceramic nanofiltration membrane for the treatment of semiconductor wastewater, Process Saf. Environ. Protect. 159 (2022) 525–533, https://doi.org/10.1016/j.psep.2022.01.032.
[41] Y. Chen, C.J. Miller, R.N. Collins, T.D. Waite, Key considerations when assessing novel Fenton catalysts: iron oxychloride (FeOCl) as a case study, Environ. Sci. Technol. 55 (2021) 13317–13325, https://doi.org/10.1021/acs.est.1c04370.
[42] Q. Wang, T.D. Lu, X.Y. Yan, L.L. Zhao, H. Yin, X.X. Xiong, R.F. Zhou, S.P. Sun, Designing nanofiltration hollow fiber membranes based on dynamic deposition technology, J. Membr. Sci. 610 (2020), 118336, https://doi.org/10.1016/j.memsci.2020.118336.
[43] B.C. Kim, J.W. Nam, K.H. Kang, Dynamic membrane filtration using powdered iron oxide for SWRO pre-treatment during red tide event, J. Membr. Sci. 524 (2017) 604–611, https://doi.org/10.1016/j.memsci.2016.11.081.
[44] P. Yao, K.H. Choo, M.H. Kim, A hybridized photocatalysis–microfiltration system with iron oxide-coated membranes for the removal of natural organic matter in water treatment: effects of iron oxide layers and colloids, Water Res. 43 (2009) 4238–4248, https://doi.org/10.1016/j.watres.2009.06.010.
[45] D.J. Miller, S. Kasemset, D.R. Paul, B.D. Freeman, Comparison of membrane fouling at constant flux and constant transmembrane pressure conditions, J. Membr. Sci. 454 (2014) 505–515, https://doi.org/10.1016/j.memsci.2013.12.027.
[46] A. Seidel, M. Elimelech, Coupling between chemical and physical interactions in natural organic matter (NOM) fouling of nanofiltration membranes: implications for fouling control, J. Membr. Sci. 203 (2002) 245–255, https://doi.org/10.1016/S0376-7388(02)00013-3.
[47] P. van den Brink, A. Zwijnenburg, G. Smith, H. Temmink, M. van Loosdrecht, Effect of free calcium concentration and ionic strength on alginate fouling in cross-flow membrane filtration, J. Membr. Sci. 345 (2009) 207–216, https://doi.org/10.1016/j.memsci.2009.08.046.
[48] S. Jiang, S. Xiao, H. Chu, J. Sun, Z. Yu, W. Zhang, Y. Chen, X. Zhou, Y. Zhang, Performance enhancement and fouling alleviation by controlling transmembrane pressure in a vibration membrane system for algae separation, J. Membr. Sci. 647 (2022), 120252, https://doi.org/10.1016/j.memsci.2022.120252.
[49] K. Akamatsu, Y. Kagami, S.I. Nakao, Effect of BSA and sodium alginate adsorption on decline of filtrate flux through polyethylene microfiltration membranes, J. Membr. Sci. 594 (2020), 117469, https://doi.org/10.1016/j.memsci.2019.117469.
[50] B. Malczewska, J. Liu, M.M. Benjamin, Virtual elimination of MF and UF fouling by adsorptive pre-coat filtration, J. Membr. Sci. 479 (2015) 159–164, https://doi.org/10.1016/j.memsci.2015.01.032.
[51] S. Zhang, T. Hedtke, Q. Zhu, M. Sun, S. Weon, Y. Zhao, E. Stavitski, M. Elimelech, J. H. Kim, Membrane-confined iron oxychloride nanocatalysts for highly efficient heterogeneous Fenton water treatment, Environ. Sci. Technol. 55 (2021) 9266–9275, https://doi.org/10.1021/acs.est.1c01391.
[52] F. Ricceri, M. Giagnorio, K.R. Zodrow, A. Tiraferri, Organic fouling in forward osmosis: governing factors and a direct comparison with membrane filtration driven by hydraulic pressure, J. Membr. Sci. 619 (2021), 118759, https://doi.org/10.1016/j.memsci.2020.118759.
[53] D.C. Sioutopoulos, A.J. Karabelas, The effect of permeation flux on the specific resistance of polysaccharide fouling layers developing during dead-end ultrafiltration, J. Membr. Sci. 473 (2015) 292–301, https://doi.org/10.1016/j.memsci.2014.09.030.
[54] J.F. Soesanto, K.J. Hwang, C.W. Cheng, H.Y. Tsai, A. Huang, C.H. Chen, T. W. Cheng, K.L. Tung, Fenton oxidation-based cleaning technology for powdered activated carbon-precoated dynamic membranes used in microfiltration seawater pretreatment systems, J. Membr. Sci. 591 (2019), 117298, https://doi.org/10.1016/j.memsci.2019.117298.
[55] D. Kuzmenko, E. Arkhangelsky, S. Belfer, V. Freger, V. Gitis, Chemical cleaning of UF membranes fouled by BSA, Desalination 179 (2005) 323–333, https://doi.org/10.1016/j.desal.2004.11.078.
[56] N. Li, Y. Tian, J. Zhao, J. Zhang, L. Kong, J. Zhang, W. Zuo, Static adsorption of protein-polysaccharide hybrids on hydrophilic modified membranes based on atomic layer deposition: anti-fouling performance and mechanism insight, J. Membr. Sci. 548 (2018) 470–480, https://doi.org/10.1016/j.memsci.2017.11.063.